Electronic changes in poly(3,4-ethylenedioxythiophene)-coated $LiFeSO_4F$ during electrochemical lithium extraction

Andreas Blidberg,[a] Mario Valvo,[a*] Maria Alfredsson,[b] Carl Tengstedt,[c] Torbjörn Gustafsson,[a] Fredrik Björefors [a]

[a] Department of Chemistry – Ångström Laboratory, Uppsala University, Box 538, SE-75121 Uppsala, Sweden

[b] School of Physical Sciences, University of Kent, CT27NH Canterbury, England

[c] Scania CV AB, SE-15187, Södertälje, Sweden.

*Corresponding author: mario.valvo@kemi.uu.se

Tel.: +46 (0)18 4713715

Keywords: Li-ion batteries; Lithium iron sulphate fluoride; Tavorite structure; X-ray absorption spectroscopy; Conductive polymers, Anionic redox processes.

Abstract

The redox activity of tavorite $LiFeSO_4F$ coated with poly(3,4-ethylenedioxythiophene), i.e. PEDOT, is investigated by means of several spectroscopic techniques. The electronic changes and iron-ligand redox features of this $LiFeSO_4F$-PEDOT composite are probed upon delithiation through X-ray absorption spectroscopy. The PEDOT coating, which is necessary here to obtain enough electrical conductivity for the electrochemical reactions of $LiFeSO_4F$ to occur, is electrochemically stable within the voltage window employed for cell cycling. Although the electronic configuration of PEDOT shows also some changes in correspondence of its reduced and oxidized forms after electrochemical conditioning in Li half-cells, its p-type doping is fully retained between 2.7 and 4.1 V with respect to Li^+/Li during the first few cycles. An increased iron-ligand interaction is observed in Li_xFeSO_4F during electrochemical lithium extraction, which appears to be a general trend for polyanionic insertion compounds.

This finding is crucial for a deeper understanding of a series of oxidation phenomena in Li-ion battery cathode materials and helps paving the way to the exploration of new energy storage materials with improved electrochemical performances.

1 Introduction

Li-ion batteries have become ubiquitous energy storage devices and revolutionized the market of portable electronics during the last decades. For the same development to occur in other areas, such as electromobility and smart grids, the energy storage capacity would need further improvements, while costs require a substantial reduction [1]. To achieve affordable charge storage devices, the latter should rely on abundant materials to decrease the production costs [2]. In terms of materials choice, it is advantageous to use iron as redox centre in positive electrodes [3], as proved by immense research interests in $LiFePO_4$ [4–6]. Traditionally, iron-based Li-ion insertion materials rely on the Fe^{3+}/Fe^{2+} redox couple [7,8], however, more exotic redox reactions are also being pursued to increase the charge storage capability. High oxidation states of iron are known for alkali ferrates and perovskite-type $AFeO_3$ ($A = Ca^{2+}$, Sr^{2+}, Ba^{2+}) [9–11], where the otherwise unstable Fe^{4+} state is stabilized by electron donation from coordinated oxygen ligands [12–14]. A similar ligand redox activity was reported upon lithium extraction in iron-based insertion materials such as $Li_{3.5}FeSbO_6$ [15], $Li_{1.19}Ti_{0.38}Fe_{0.43}O_2$ [16], α-$NaFeO_2$ [17] and Li_2FeSiO_4 [18].

Anionic contributions to the redox activity of Li-rich layered oxides have also attracted considerable attention [19–21]. The redox activity of Li-ion insertion compounds based on polyatomic anions (XO_n^{m-} with X = B, Si, P, S, etc., referred to as “polyanions”), however, has not yet received the same degree of attention. In polyanionic compounds, the Fe-O bond is more ionic than that of transition metal oxides, since the electrons are pulled away from the transition metal by the ‘inductive effect’ in the Fe-O-X linkage [22]. The transition metal has

typically been considered the sole contributor to the redox activity of these compounds due to limited covalence of the Fe-O bond. However, studies on iron- and cobalt phosphates have shown electronic changes also for the phosphate anion [23–26]. As extreme example, the manganese in $LiMnPO_4$ hardly showed any redox activity during lithium extraction [27]. Also oxyphosphates, sulphates and molybdates exhibited more complicated electronic changes during oxidation than a pure Fe^{3+}/Fe^{2+} activity [28,29]. Moreover, alluaudite-type $Na_{2.56}Fe_{1.72}(SO_4)_3$, a promising cathode material for Na-ion batteries, displayed an oxygen contribution to its redox activity [30]. Clearly, the redox reactions of polyanionic insertion materials are accompanied by complex electronic rearrangements in addition to expected electronic changes in the transition metal. A deeper understanding of these electronic changes in polyanionic insertion compounds, in turn, should aid the development of new materials with improved energy storage capacities.

$LiFeSO_4F$ crystallizes into two different polymorphs, tavorite- and triplite-type, depending on the synthesis conditions [31–33]. The tavorite-type offers a decent energy storage capacity with an open crystal framework providing fast solid-state Li-ion transport [31,34]. It shows minimal polarization upon electrochemical cycling when coated with p-doped PEDOT [35], since this alleviates a kinetic barrier for its lithium insertion/extraction reactions [36], similarly to carbon coatings [61] or foams [62] applied to $LiFePO_4$. Both $LiFeSO_4F$ and PEDOT are electrochemically active at overlapping potentials, thus making the study of the electronic changes in this composite very intriguing. The p-doping process of PEDOT starts at ≈2.5 V vs. Li^+/Li and spans over a wide potential range [37], while tavorite-type $LiFeSO_4F$ shows a characteristic redox activity around 3.6 V vs. Li^+/Li [31].

Herein, we expand the understanding of composite materials for electrochemical charge storage based on this tavorite-type $LiFeSO_4F$ insertion compound and the conductive polymer poly(3,4-ethylenedioxythiophene) (PEDOT). A combination of S and Fe K-edge X-ray

Absorption Near Edge Spectroscopy (XANES) together with Raman and ^{57}Fe Mössbauer spectroscopies is utilised here to accurately track the electronic changes in PEDOT-coated $LiFeSO_4F$ upon electrochemical oxidation and associated Li^+ extraction.

2 Experimental

Tavorite-type lithium iron sulphate fluoride ($LiFeSO_4F$) was synthesized by solvothermal synthesis [54] under the same conditions earlier reported by Sobkowiak et al. [55]. The precursors were $FeSO_4 \cdot H_2O$ (prepared by dehydration of $FeSO_4 \cdot 7H_2O$, ≥99.0% Sigma-Aldrich) and LiF (99.85%, Alfa-Aesar). Tetraethylene glycol (99%, Aldrich) was used as reaction medium in a Teflon-lined steel autoclave (Parr Instruments). $LiFeSO_4F$ was coated with p-doped poly(3,4-ethylenedioxythiophene)-bis(trifluoromethane)sulfonimide (PEDOT-TFSI) via a synthetic route originally developed for coating $LiFePO_4$ [56] under the same conditions reported elsewhere [35]. Details about the synthesis of p-doped PEDOT can be found in refs. [35,36,56,60]. The chemicals used for this purpose were NO_2BF_4 (>95%, Aldrich), 3,4-ethylenedioxythiophene (97%, Sigma-Aldrich), LiTFSI (Purolyte, Ferro, dried in vacuum at 120 °C for 10 h), methanol (99.8%, anhydrous, Sigma-Aldrich), acetonitrile (99.8%, anhydrous, Sigma-Aldrich) and acetone (99.8%, anhydrous, WVR). A reference sample of uncoated $Li_{0.1}FeSO_4F$ (i.e. delithiated) was obtained by suspension in acetonitrile and NO_2BF_4 under overnight stirring. Reference p-doped PEDOT samples (labelled later as PEDOT-TFSI) were prepared similarly to $LiFeSO_4F$-PEDOT composites, yet with anhydrous $FeCl_3$ (>98.0%, Merck) as oxidizing agent. The polymer was washed several times with acetonitrile and methanol and dried under vacuum at 120 °C overnight.

$LiFeSO_4F$-PEDOT composites were thoroughly mixed in an agate mortar only with carbon black (Super P, Erachem) and no binder inside an argon-filled glovebox (M-Braun) prior to electrochemical conditioning. Swagelok-type cells were assembled with a typical mass

loading of ≈30 mg of $LiFeSO_4F$-PEDOT/carbon mixture pushed onto an Al current collector. No carbon additive was used for the PEDOT references. A lithium metal disc on a Ni current collector was used as counter- and reference electrode. 1 M $LiPF_6$ in ethylene carbonate and diethyl carbonate (EC-DEC) in a 1:1 volume ratio (i.e. LP40, BASF) was used as electrolyte. The latter was infiltrated through glass fibre separators (Whatman, GE Healthcare), while a stainless steel spring ensured stack pressure in the cells. Cell assembly was performed in an argon-filled glovebox with moisture and oxygen levels below 1 ppm. Galvanostatic cycling was run on a Novonix high precision charging system at a constant temperature of 30 °C.

X-ray Absorption Near Edge Spectroscopy (XANES) was performed at the European Synchrotron Radiation Facility (ESRF) at the BM 28–XMaS beamline. A double-crystal silicon (111) monochromator operated in focused mode was used to tune the energy of the X-ray beam. The samples were measured under He flow and incoming photon flux was monitored by measuring the fluorescence from a Ni grid with a Vortex Si Drift Detector (SDD). The signals were collected in fluorescence mode with a Ketek SDD. The beam was aligned at 2472 eV for sulphur K-edge and at 7112 eV for iron K-edge measurements. Data collection was performed between 2450-2520 eV for sulphur and 7090-7170 eV for iron, respectively. Data processing was run with the Athena software [57] and the main absorption edge was extracted from the maximum first derivative. Powder X-ray diffraction (XRD) was carried out on a Bruker D8 Advance diffractometer with Cu $K\alpha_{1,2}$ radiation and a LYNXEYE-XE line detector. Structural refinements were performed through the Rietveld method [58] using the FullProf software [59]. Mössbauer spectra were collected from circular absorber discs (d = 13 mm) typically consisting of ≈30 mg of $LiFeSO_4F$ mixed with an inert boron nitride filler. The measurements were run in transmission mode using a ^{57}Co<u>Rh</u> source at constant acceleration. The spectra were Lorentzian line least-squares fitted using the Recoil software and reported with respect to a metallic iron (α-Fe) reference measured at room

temperature (RT). Raman spectra were collected with a Renishaw InVia spectrometer from 100 to 2000 cm^{-1} through 20 cumulative acquisitions having a measuring time of 20 s and a constant nominal laser power ≤0.5 mW. The instrument was calibrated taking as reference peak the signal at 520.6 cm^{-1} from a Si wafer. Excitation wavelengths of 532, 633 and 785 nm, generated respectively by He-Ne (633 nm) and solid-state diode (532, 785 nm) lasers (Renishaw), were utilized, while beam exposure of the samples was minimized to avoid materials degradation. Fourier transform infrared (FT-IR) spectroscopy was carried out in attenuated total reflectance (ATR) mode on a PerkinElmer Spectrum One spectrometer with a diamond window. FT-IR spectra were recorded through 20 cumulative scans between 4000 and 560 cm^{-1} with a resolution of 4 cm^{-1}. Thermogravimetric analysis (TGA) was performed on a Q500 TA Instruments equipment in ramping mode using an aluminium pan and a heating rate of 5 °C min^{-1} from RT to 600 °C under a constant airflow.

3 Results and discussion

Fig. 1 shows the characterization of the $LiFeSO_4F$-PEDOT composite. Rietveld refinement of the $LiFeSO_4F$ XRD pattern showed 94 wt.% purity for this compound, with only small amounts of $FeSO_4 \cdot H_2O$ and LiF precursors still present. The Raman spectrum of $LiFeSO_4F$-PEDOT clearly displayed a series of characteristic vibration modes for PEDOT (Fig. 1b) [38–40]. A moderate quantity of PEDOT was aimed here to achieve convenient signal-to-noise ratios from both constituents of the $LiFeSO_4F$-PEDOT composite during vibrational spectroscopy analyses. Quantification by TGA proved that 23.5 wt.% PEDOT was present in the composite (Fig. 1c).

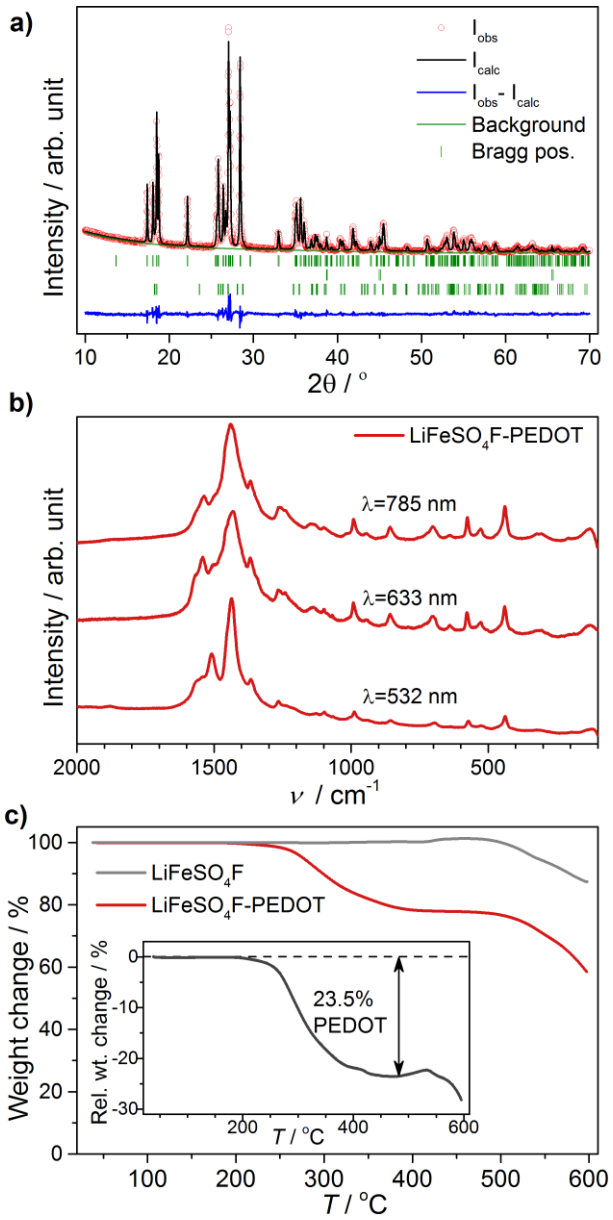

Fig. 1. Structural, vibrational and thermal characterization of the $LiFeSO_4F$-PEDOT composite. a) Rietveld refinement of the XRD pattern of $LiFeSO_4F$ with highlighted characteristic Bragg diffractions corresponding (from the top to bottom) to those of $LiFeSO_4F$, LiF and $FeSO_4{\cdot}H_2O$, respectively. b) Raman spectra of $LiFeSO_4F$-PEDOT obtained with different excitation wavelengths. c) Quantification of the PEDOT coating content by means of TGA measurements. More details about the crystal structure and purity of tavorite $LiFeSO_4F$ can be found in refs. [36,55]. Note that PEDOT undergoes Resonant Raman Scattering (RRS) at all the excitation wavelengths.

In addition to the $LiFeSO_4F$-PEDOT composite, samples of $LiFeSO_4F$ and PEDOT with different degrees of oxidation were separately prepared. These specimens were used as key references in the XANES analysis of the $LiFeSO_4F$-PEDOT composites and their

characterizations are presented in Fig. 2. ^{57}Fe Mössbauer spectroscopy of pristine $LiFeSO_4F$ showed no traces of contamination due to Fe^{3+}-containing compounds (Fig. 2a). Chemical oxidation by NO_2BF_4 resulted in a nearly complete extraction of lithium, as 90 mol.% Fe^{3+} was consequently present in the sample (Fig. 2b). The XRD patterns of these phases corresponded to $LiFeSO_4F$ for the pristine sample, while mainly to $FeSO_4F$ for the chemically oxidized one [31] (Fig. S1 in Supporting Information – SI). Surprisingly, the sulphur K-edge XANES spectra of Li_xFeSO_4F displayed interesting differences for the various degrees of lithiation (x = 1, 0.1 from the Mössbauer analyses). Upon delithiation, a pre-edge appeared accompanied by a 0.7 eV shift of the main absorption edge towards higher energies (Fig. 2c). These features were also observed in electrochemically oxidized $LiFeSO_4F$-PEDOT composites, as discussed later. Reference p-doped PEDOT samples were prepared by using $FeCl_3$ as oxidizing agent, instead of the partly oxidized Li_xFeSO_4F, which was employed for the preparation of the $LiFeSO_4F$-PEDOT composites [35]. The Raman spectra of the as-synthesized PEDOT reference were almost identical to that of the $LiFeSO_4F$-PEDOT (Fig. S2, SI). Different doping levels were obtained for PEDOT by galvanostatic cycling and stopping of the cells at different potentials after a few charge/discharge cycles (Fig. 2d). The charge on oxidation (i.e. delithiation) corresponded to a doping level of +0.35, based on the PEDOT weight and the $TFSI^-$ counterion, in line with previous values for stable electrochemical performance [41,42]. The Raman spectra of these cycled samples displayed some clear differences (Fig. 2e). The strong band around 1430 cm^{-1} (assigned to $C_\alpha=C_\beta$ stretching) was broadened after charging to 3.65 V, thereby indicating PEDOT oxidation [38,40]. Resonant Raman scattering (RRS) of PEDOT, due to a series of electronic transitions occurring from the visible to near-infrared regions, resulted in complex spectra. The π-π^* electronic transition is centred around 600 nm for neutral PEDOT and around 850 nm for its

p-doped form [38,43]. Nevertheless, the RRS can be used to qualitatively probe the degree of oxidation of PEDOT.

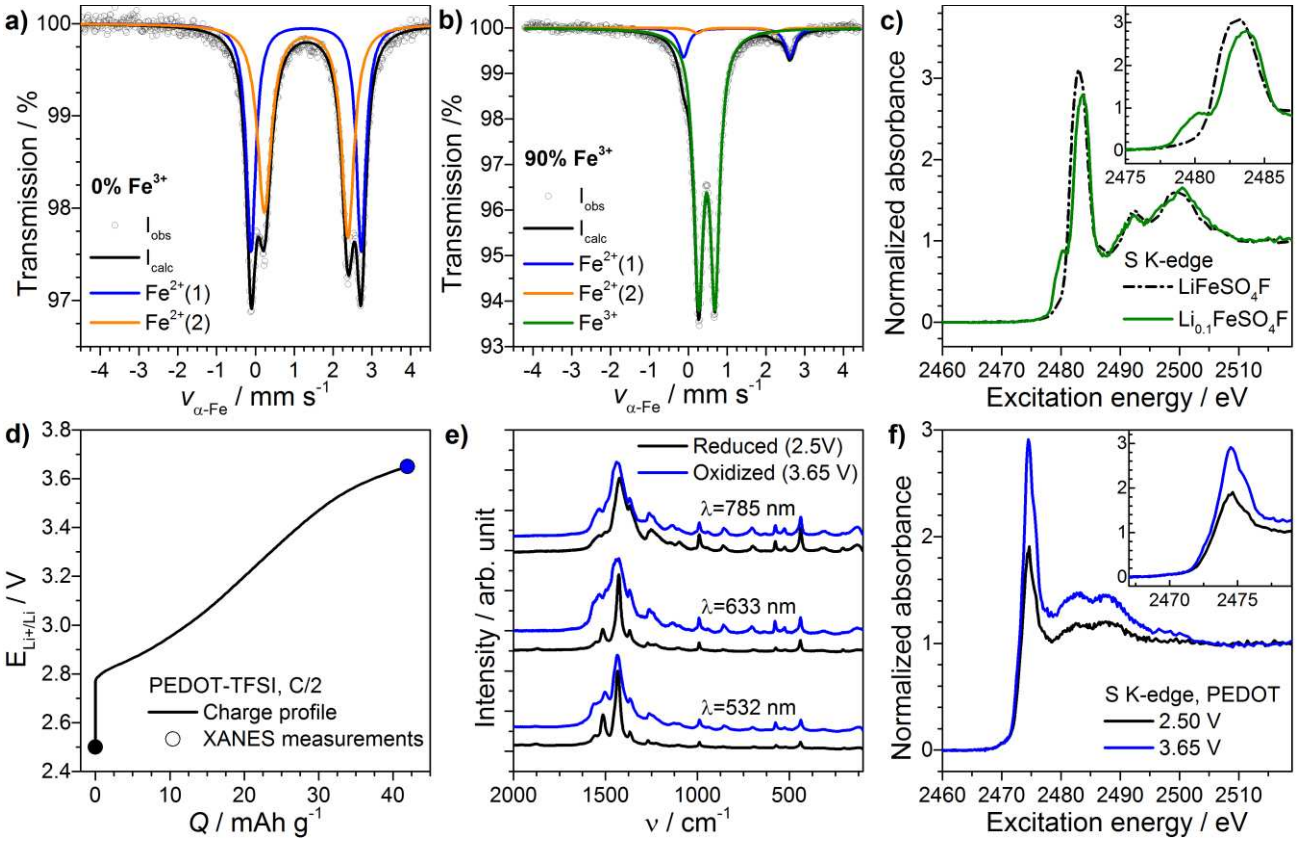

Fig. 2. Individual characterization of $LiFeSO_4F$ and PEDOT references. Mössbauer spectroscopy of a) $LiFeSO_4F$ reference and b) chemically oxidized $Li_{0.1}FeSO_4F$. c) S K-edge XANES for both $LiFeSO_4F$ and $Li_{0.1}FeSO_4F$. d) Electrochemical conditioning of originally p-doped PEDOT references (i.e. 'PEDOT-TFSI') cycled in Li half-cells with a $LiPF_6$ electrolyte and associated e) normalized Raman spectra and f) S K-edge XANES spectra with magnified spectral range around their peak maxima (inset). Note that p-doping of PEDOT in Fig. 2d holds mainly at high voltages (e.g. >2.7 V vs. Li^+/Li), while other negatively charged counterions (e.g. $(PF_6)^-$) can also contribute to charge balancing via possible ion exchange with $TFSI^-$ [36].

The broadening around 1430 cm^{-1} was amplified by measuring with longer wavelengths closer to the π-π* transition of p-doped PEDOT [38]. This observation confirmed a successful p-doping of the PEDOT. Despite these clear differences in the Raman spectra, characteristic vibrations of p-doped PEDOT were still observed in the FT-IR spectra for both samples (Fig. S3, SI). The IR-active vibrations differ only in intensity for different doping levels [44] and

the PEDOT reference samples showed a clear variation in the degree of doping according to the electrochemical and Raman analyses. The sulphur K-edge XANES spectra for nearly neutral and fully p-doped PEDOT (i.e. charged to 3.65 V) highlighted a difference in normalized absorption with an increased relative intensity at the main absorption edge for the p-doped specimen (Fig. 2f). This higher absorbance for p-doped PEDOT could be due to enhanced delocalization of the electronic states in a more conjugated form of p-doped polymer [38,45] with increased electron density on the sulphur atom. The spectra are similar to that of poly(3-methylthiophene), whose absorption peaks have been assigned earlier [46].

Fig. 3 shows the S and Fe K-edge spectra for $LiFeSO_4F$-PEDOT composites oxidized to different potentials. All the samples were pre-cycled galvanostatically at C/10 and conditioned at 2.5 V vs. Li^+/Li until the current dropped and corresponded to C/50. Almost identical representative behaviours were observed for all the cells (Fig. S4, SI). Two $LiFeSO_4F$-PEDOT electrodes were oxidized to different potentials at a C/10 rate after the first few cycles (Fig. 3a). One cell was stopped at the beginning of the voltage plateau (3.59 V) and another one at the end of the charge (4.1 V). 83% of the theoretical capacity was extracted (based on the specific capacities of $LiFeSO_4F$ and PEDOT-TFSI, respectively), thus providing a value slightly lower than that obtained via its similar chemical oxidation. The Fe K-edge spectrum exhibited a clear shift of the absorption edge towards higher energies upon oxidation (Fig. 3b). This shift is related to the conversion of Fe^{2+} to Fe^{3+}, which was also observed by ^{57}Fe Mössbauer spectroscopy for the Li_xFeSO_4F reference samples. The S K-edge spectra (Fig. 3c) displayed a combination of the signals individually recorded for the pure $LiFeSO_4F$ and p-doped PEDOT reference samples (Fig. 2c and f), while the absorption edge for the PEDOT was well separated from that of $LiFeSO_4F$ in all the specimens. An attempt to distinguish the individual contributions of $LiFeSO_4F$ and PEDOT required a linear combination fitting of the S K-edge spectrum for the $LiFeSO_4F$-PEDOT composite (Fig. S5,

SI). This fitting procedure resulted in 76.4% of $LiFeSO_4F$ and 23.6% of p-doped PEDOT, i.e. the same composition earlier obtained in an independent way by TGA (see Fig. 1c and Fig. S5, SI), thus agreeing well with this complementary analysis. The PEDOT signal was present in all the samples, showing that over-oxidation did not occur even at the highest potential. When present, oxidative degradation of PEDOT leads to the formation of sulfonyl groups [47] giving rise to a less intense tiophene sulphur signal [48]. The main absorption edge for the PEDOT signal was at 2474.0 eV, similarly to the p-doped reference sample, while no intensity change for this feature was observed for the electrodes charged at different potentials. These results imply that the PEDOT was p-doped in all the three cases, which is beneficial for both electronic conductivity [39] and overall electrochemical performance. These findings match well also with previous XPS studies on $LiFeSO_4F$-PEDOT composites [36].

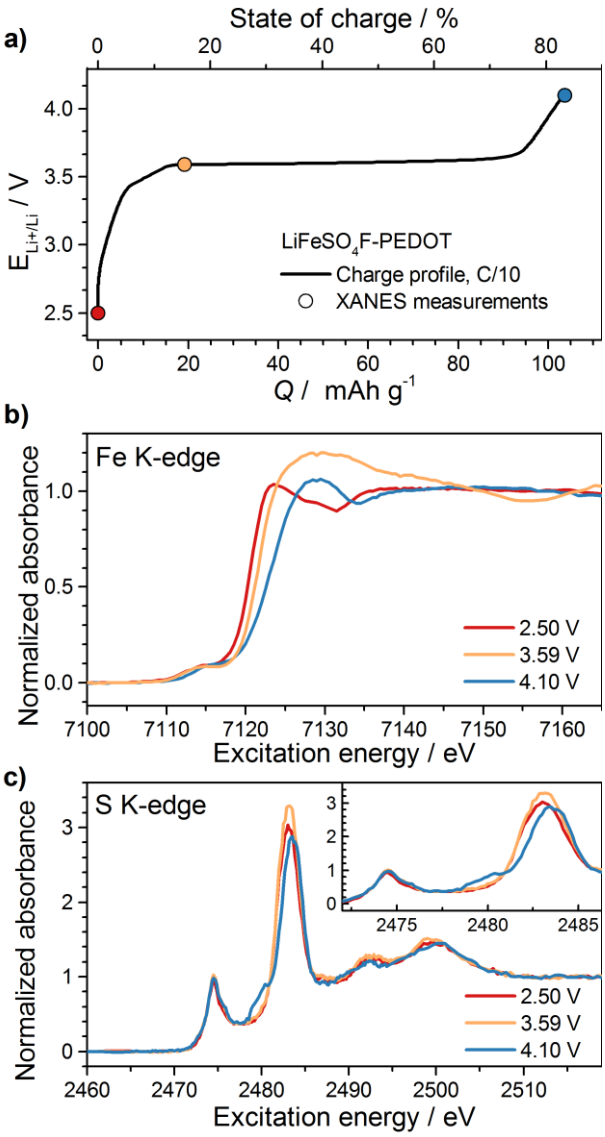

Fig. 3. XANES analysis of $LiFeSO_4F$-PEDOT composites after galvanostatic cycling to different voltages in three separate Li half-cells. a) Representative voltage points in the charge profile associated with distinctive states of lithiation for the corresponding electrodes which were analysed by means of XANES. b) Fe K-edge and c) S K-edge spectra for the same composite electrode samples. Note the changes in both Fe and S K-edges and the appearance of a pre-edge feature for the sulphate group at 2480 eV in c) for the specimen charged to the highest voltage (see also magnified inset). The change of normalized peak absorption with varying electrode potential in b) and c) refers only to the representative voltage points indicated in a).

It is worth mentioning that partial PEDOT re-oxidation might have occurred due to incomplete lithiation of $LiFeSO_4F$ in the composite. However, complete discharge to 2.5 V during near-equilibrium conditions (C/50) and rapid disassembly of the cells should prevent

PEDOT re-oxidation. A pre-edge appeared for $LiFeSO_4F$ in the S K-edge spectrum also during electrochemical oxidation, analogously to its chemical delithiation, and was accompanied by a shift of the absorption edge to 0.9 eV towards higher energies. A similar feature was noticed previously for anhydrous $CuSO_4$ [49] with a main absorption edge at higher energies than $ZnSO_4$, which lacked this pre-edge. A comparable pre-edge was also found in the S K-edge and P K-edge spectra of $Fe_2(SO_4)_3$ and $Li_3Fe_2(PO_4)_3$, respectively, while this feature disappeared upon lithium insertion [23,29]. However, no drastic changes were observed in the O K-edge for $Fe_2(SO_4)_3$ and such pre-edge features were assigned to electrostatic interactions with inserted Li-ions, similarly to $LiCoPO_4$ [25,50]. Therefore, control measurements on anhydrous ferrous- and ferric iron sulphates in absence of lithium were performed here as well (Fig. S6, SI). The pre-edge was observed in the S K-edge spectrum for $Fe_2(SO_4)_3$, yet not for $Fe(SO_4)$. The absence of lithium in these compounds and the similarities with the S K-edge features of Li_xFeSO_4F would then contradict the view that the changes in the S K-edge spectra could be due to electrostatic interactions with lithium. Additionally, hybridization of the Fe 3d and O 2p orbitals was observed with O K-edge XANES for alluaudite-type $Na_{2.56}Fe_{1.72}(SO_4)_3$ upon oxidation, whereas purely ionic Fe^{2+} was detected for pristine samples [30]. The electronic density of states for both $Na_{2.56}Fe_{1.72}(SO_4)_3$ and $LiFeSO_4F$ showed increased hybridization between the spin-down Fe 3d states and the sulphur and oxygen sp states [30,51,52]. Indeed, Bader charge analysis (i.e. calculation of electronic charges on individual atoms in the crystal) demonstrated that iron accounted only for 43% of the increased charge in $Na_{2.56}Fe_{1.72}(SO_4)_3$ upon desodiation, whereas 57% in $LiFeSO_4F$ upon lithium extraction [30,53]. The remaining charge was compensated by the coordinated ligands. These combined analyses of tavorite-type $LiFeSO_4F$ together with previous reports on polyanionic compounds indicate that an increased iron-ligand interaction

can be a general trend upon oxidation from Fe^{2+} to Fe^{3+}, as commonly observed for the higher Fe^{4+} oxidation state [13–18].

Conclusions

The changes in the electronic structure of tavorite-type $LiFeSO_4F$ coated with PEDOT were carefully investigated through S and Fe K-edge XANES, Mössbauer and Raman spectroscopies. The PEDOT coating remained practically p-doped in the potential range of 2.5-4.1 V vs. Li^+/Li during the initial cycles, demonstrating a favourable electrochemical stability and electronic conductivity in the $LiFeSO_4F$-PEDOT composite. Increased iron-ligand electronic interaction observed during lithium extraction appears to be a general feature for iron sulphates and phosphates. In a wider perspective, this finding is essential for a thorough understanding of oxidation phenomena in insertion-type materials and thus valuable for pursuing enhanced charge storage capabilities based on a simultaneous redox activity of both transition metal centres and coordinated ligands.

Acknowledgements

Lennart Häggström and Tore Ericsson are acknowledged for excellent support regarding Mössbauer measurements, Paul Thompson, Marcus Bertuzzo and Nanami Yokota for assistance with practical and theoretical issues surrounding XANES. The beamtime at the EPSRC-funded XmaS beamline (BM28) at the European Synchrotron Radiation Facility (ESRF) was greatly appreciated. The Swedish Foundation for Strategic Research (SSF) is also acknowledged for funding through the project “From road to load”. Additional support by the Swedish strategic research program “StandUp for Energy” is also acknowledged. M. Valvo gratefully acknowledges the financial support of the Swedish Research Council (FORMAS)

via the personal grant no. 245-2014-668, as well as that by the Swedish Energy Agency (grant. no. 2017-013531) and Åforsk Foundation (grant. no. 18-317).

References

[1] G. E. Blomgren, J. Electrochem. Soc. 164 (2017) A5019–A5025.

[2] E. J. Berg, C. Villevieille, D. Streich, S. Trabesinger, P. Novák, J. Electrochem. Soc. 162 (2015) A2468–A2475.

[3] A. Yamada, MRS Bull. 39 (2014) 423–428.

[4] A. K. Padhi, K. S. Nanjundaswamy, J. B. Goodenough, J. Electrochem. Soc. 144 (1997) 1188–1194.

[5] L.-X. Yuan, Z.-H. Wang, W.-X. Zhang, X.-L. Hu, J.-T. Chen, Y.-H. Huang, J. B. Goodenough, Energy Environ. Sci. 4 (2011) 269–284.

[6] J. Wang, X. Sun, Energy Environ. Sci. 8 (2015) 1110–1138.

[7] A. Gutierrez, N. A. Benedek, A. Manthiram, Chem. Mater. 25 (2013) 4010–4016.

[8] C. Masquelier, L. Croguennec, Chem. Rev. 113 (2013) 6552–6591.

[9] J. B. MacChesney, R. C. Sherwood, J. F. Potter, J. Chem. Phys. 43 (1965) 1907–1913.

[10] F. Kanamaru, H. Miyamoto, Y. Mimura, M. Koizumi, M. Shimada, S. Kume, S. Shin, Mater. Res. Bull. 5 (1970) 257–261.

[11] H. J. Van Hook, J. Phys. Chem. 68 (1964) 3786–3789.

[12] J. Zaanen, G. A. Sawatzky, J. W. Allen, Phys. Rev. Lett. 55 (1985) 418–421.

[13] A. E. Bocquet, A. Fujimori, T. Mizokawa, T. Saitoh, H. Namatame, S. Suga, N. Kimizuka, Y. Takeda, M. Takano, Phys. Rev. B 45 (1992) 1561–1570.

[14] N. Hayashi, T. Yamamoto, H. Kageyama, M. Nishi, Y. Watanabe, T. Kawakami, Y. Matsushita, A. Fujimori, M. Takano, Angew. Chemie Int. Ed. 50 (2011) 12547–12550.

[15] E. McCalla, M. T. Sougrati, G. Rousse, E. J. Berg, A. Abakumov, N. Recham, K. Ramesha, M. Sathiya, R. Dominko, G. Van Tendeloo, P. Novák, J.-M. Tarascon, J. Am. Chem. Soc. 137 (2015) 4804–4814.

[16] S. L. Glazier, J. Li, J. Zhou, T. Bond, J. R. Dahn, Chem. Mater. 27 (2015) 7751–7756.

[17] E. Lee, D. E. Brown, E. E. Alp, Y. Ren, J. Lu, J.-J. Woo, C. S. Johnson, Chem. Mater. 27 (2015) 6755–6764.

[18] T. Masese, C. Tassel, Y. Orikasa, Y. Koyama, H. Arai, N. Hayashi, J. Kim, T. Mori, K. Yamamoto, Y. Kobayashi, H. Kageyama, Z. Ogumi, Y. Uchimoto, J. Phys. Chem. C 119 (2015) 10206–10211.

[19] K. Luo, M. R. Roberts, R. Hao, N. Guerrini, D. M. Pickup, Y.-S. Liu, K. Edström, J. Guo, A. V. Chadwick, L. C. Duda, P. G. Bruce, Nat. Chem. 8 (2016) 684–691.

[20] D.-H. Seo, J. Lee, A. Urban, R. Malik, S. Kang, G. Ceder, Nat. Chem. 8 (2016) 692–697.

[21] A. Grimaud, W. T. Hong, Y. Shao-Horn, J.-M. Tarascon, Nat. Mater. 15 (2016) 121–126.

[22] A. K. Padhi, J. Electrochem. Soc. 145 (1998) 1518-1520.

[23] J. Shirakawa, M. Nakayama, M. Wakihara, Y. Uchimoto, J. Phys. Chem. B 110 (2006) 17743–17750.

[24] M. Nakayama, S. Goto, Y. Uchimoto, M. Wakihara, Y. Kitajima, Chem. Mater. 16 (2004) 3399–3401.

[25] M. Nakayama, S. Goto, Y. Uchimoto, M. Wakihara, Y. Kitajima, T. Miyanaga, I. Watanabe, J. Phys. Chem. B 109 (2005) 11197–11203.

[26] A. Augustsson, G. V. Zhuang, S. M. Butorin, J. M. Osorio-Guillén, C. L. Dong, R. Ahuja, C. L. Chang, P. N. Ross, J. Nordgren, J.-H. Guo, J. Chem. Phys. 123 (2005) 184717-1 – 184717-9.

[27] H. M. Hollmark, T. Gustafsson, K. Edström, L.-C. Duda, Phys. Chem. Chem. Phys. 13 (2011) 20215–20222.

[28] H. M. Hollmark, K. Maher, I. Saadoune, T. Gustafsson, K. Edström, L.-C. Duda, Phys. Chem. Chem. Phys. 13 (2011) 6544–6551.

[29] J. Shirakawa, M. Nakayama, M. Wakihara, Y. Uchimoto, J. Phys. Chem. B 111, (2007) 1424–1430.

[30] G. Oyama, H. Kiuchi, S. C. Chung, Y. Harada, A. Yamada, J. Phys. Chem. C 120 (2016) 23323–23328.

[31] N. Recham, J.-N. Chotard, L. Dupont, C. Delacourt, W. Walker, M. Armand, J.-M. Tarascon, Nat. Mater. 9 (2010) 68–74.

[32] P. Barpanda, M. Ati, B. C. Melot, G. Rousse, J.-N. Chotard, M.-L. Doublet, M. T. Sougrati, S. A. Corr, J.-C. Jumas, J.-M. Tarascon, Nat. Mater. 10 (2011) 772–779.

[33] L. Liu, B. Zhang, X. Huang, Prog. Nat. Sci. Mater. Int. 21 (2011) 211–215.

[34] R. Tripathi, G. R. Gardiner, M. S. Islam, L. F. Nazar, Chem. Mater. 23 (2011) 2278–2284.

[35] A. Sobkowiak, M. R. Roberts, R. Younesi, T. Ericsson, L. Häggström, C.-W. Tai, A. M. Andersson, K. Edström, T. Gustafsson, F. Björefors, Chem. Mater. 25 (2013) 3020–3029.

[36] A. Blidberg, A. Sobkowiak, C. Tengstedt, M. Valvo, T. Gustafsson, F. Björefors. ChemElectroChem 4 (2017) 1896–1907.

[37] C. Kvarnström, H. Neugebauer, S. Blomquist, H. J. Ahonen, J. Kankare, A. Ivaska, Electrochim. Acta 44 (1999) 2739–2750.

[38] S. Garreau, G. Louarn, J. P. Buisson, G. Froyer, S. Lefrant, Macromolecules, 32 (1999) 6807–6812.

[39] W. W. Chiu, J. Travaš-Sejdić, R. P. Cooney, G. A. Bowmaker, Synth. Met. 155 (2005) 80–88.

[40] G. Louarn, J. P. Buisson, S. Lefrant, D. Fichou, J. Phys. Chem. 99 (1995) 11399–11404.

[41] F. Jonas, G. Heywang, W. Schmidtberg, J. Heinze, M. Dietrich, EP0339340 (A2) (1989).

[42] C. Arbizzani, M. Mastragostino, M. Rossi, Electrochem. Commun. 4 (2002) 545–549.

[43] J. C. Gustafsson-Carlberg, O. Inganäs, M. R. Andersson, C. Booth, A. Azens, C. G. Granqvist, Electrochim. Acta 40 (1995) 2233–2235.

[44] C. Kvarnström, H. Neugebauer, A. Ivaska, N. Sariciftci, J. Mol. Struct. 521 (2000) 271–277.

[45] A. Lenz, H. Kariis, A. Pohl, P. Persson, L. Ojamäe, Chem. Phys. 384 (2011) 44–51.

[46] G. Tourillon, A. M. Flank, P. Lagarde, J. Phys. Chem. 92 (1988) 4397–4400.

[47] P. Tehrani, A. Kanciurzewska, X. Crispin, N. D. Robinson, M. Fahlman, M. Berggren, Solid State Ionics 177 (2007) 3521–3527.

[48] I. Winter, C. Reese, J. Hormes, G. Heywang, F. Jonas, Chem. Phys. 194 (1995) 207–213.

[49] R. K. Szilagyi, P. Frank, S. DeBeer George, B. Hedman, K. O. Hodgson, Inorg. Chem. 43 (2004) 8318–8329.

[50] O. Le Bacq, A. Pasturel, O. Bengone, Phys. Rev. B 69 (2004) 245107-1 – 245107-10.

[51] S. C. Chung, P. Barpanda, S.-I. Nishimura, Y. Yamada, A. Yamada, Phys. Chem. Chem. Phys. 14 (2012) 8678-8682.

[52] Y. Cai, G. Chen, X. Xu, F. Du, Z. Li, X. Meng, C. Wang, Y. Wei, J. Phys. Chem. C 115 (2011) 7032–7037.

[53] M. Ramzan, S. Lebègue, T. W. Kang, R. Ahuja, J. Phys. Chem. C 115 (2011) 2600–2603.

[54] R. Tripathi, T. N. Ramesh, B. L. Ellis, L. F. Nazar, Angew. Chem. Int. Ed. 49 (2010) 8738–8742.

[55] A. Sobkowiak, M. R. Roberts, L. Häggström, T. Ericsson, A. M. Andersson, K. Edström, T. Gustafsson, F. Björefors, Chem. Mater. 26 (2014) 4620–4628.

[56] D. Lepage, C. Michot, G. Liang, M. Gauthier, S. B. Schougaard, Angew. Chemie Int. Ed. 50 (2011) 6884–6887.

[57] B. Ravel, M. Newville, J. Synchrotron Radiat. 12 (2005) 537–541.

[58] H. M. Rietveld, J. Appl. Crystallogr. 2 (1969) 65–71.

[59] J. Rodríguez-Carvajal, Phys. B Condens. Matter 192 (1993) 55–69.

[60] S. Kirchmeyer, K. Reuter, J. Mater. Chem. 15 (2005) 2077–2088.

[61] N. Ravet, Y. Chouinard, J. F. Magnan, S. Besner, M.Gauthier, M. Armand, J. Power Sources 97–98 (2001) 503–507.

[62] H. D. Asfaw, M. R. Roberts, C.-W. Tai, R. Younesi, M. Valvo, L. Nyholm, K. Edström, Nanoscale 6 (2014) 8804–8813.